Acknowledgements

Throughout the duration of my project, I have been given the opportunity to work with and learn from a number of people. I am indebted to my supervisor, [redacted] who supervised and directed me whenever I was uncertain or in doubt of certain theories. Many thanks to [redacted] for assisting in the experimentation of some of the components and for the helpful comments made regarding the use of AWR Microwave Office, crucial to completing the project. [redacted]., and the members of electronic services were very helpful in seeing to it that my microstrip designs were carefully fabricated. I would also like to thank [redacted] for teaching me to use ADS another key RF design software and [redacted] for his advice on designing a working 6-Element Yagi Antenna, for all these, I am very grateful.

Abstract

The acronym RADAR (radio, detection and ranging) suggests that early radars were primarily designed to provide the operator with range information of a target. Various techniques are used to design a radar, depending on the intended application. Essentially, they are used to detect the presence of a target, its altitude in space, size, shape, velocity and direction of motion or even its identity.

This report focuses on the Frequency Modulation-Continuous-wave radar type although other radar types are discussed. All design methods and microwave circuit design techniques used to fabricate all the radar components, present in the system's block diagram, are outlined. For the purchased system elements, their modes of operation are described.

Test results of the component parts and the integrated systems are presented. In addition, the block diagram of Gary Haikney, an ex-student who worked on a similar project previously, was redesigned; some of the existing components following testing were re-fabricated to correct detected and predicted errors that might have led to the malfunctioning of its design.

Contents

List of Tables, Figures and Constants

Constant	Symbol	Value
RT Duroid 5880 Characteristics		
Dielectric constant	ε_r	2.2 ± 0.015
Loss Tangent	$\tan \delta$	0.0009
Height of dielectric	h	787µm
Thickness of Conductor	Th	17.5µm
Speed of Light	c	$3x10^8$m/s
Other Constants		
Boltzmann constant	K	$1.38 \times 10^{-23}JK^{-1}$
Room Temperature	T	290K
Permittivity of Space	ε_0	8.85×10^{-12} F/m
Radar cross section {of car}	σ	100

1 Introduction

A radar is an electromagnetic system used for the detection and location of objects known as targets. When in operation, a primary radar transmits a waveform with known characteristics before comparing this transmitted waveform with its corresponding reflection or echo to obtain a difference signal which could be in form of an error signal or delay. This difference signal is then used to stir the servo of a tracker or provide range information depending on if the radar is for tracking or search purposes; Primary radars such as FMCW radars for instance, rely on such echoes to provide target information whereas secondary radars rely on responses of the target to incident 'interrogative' signals via a transponder placed on its target.

Many scientists have contributed to the development of the radar. The technology dates back to 1886 when Heinrich Hertz illustrated the possibility of radio waves reflecting off the surfaces of metallic and dielectric bodies. In 1903, Christian Hulsmeyer went on to demonstrate the feasibility of detecting the presence of a ship in dense fog using his telemobiloscope and eventually got a patent protecting this in 1904. Marconi in 1922, recognised the potential of the short waves initially experimented by Heinrich Hertz; He observed that apart from being reflected from conducting bodies, they were also suitable for radio detection to give information such as the presence or bearing of a target. The US Naval Research Laboratory and Bell laboratory have also contributed to making it a full-fledged technology and till date, through research and implementation of related projects, more ideas have risen to develop the technology even further [1].

Radars usually operate between 300MHz to 15GHz; they generate RF fields which are known to interact differently with the human body. The depth of penetration of the waves in human tissues being greater for lower frequencies below 10GHz. A specific absorption rate (SAR) of at least 4W/Kg is needed to produce known adverse health effects. To achieve an SAR of lower than 4W/Kg, the radar should have good directionality enabling RF levels away from the main beam fall off. Researchers till date, do not have evidence that adverse health effect arise as a result of repeated exposure to low level RF fields [2]. Consequently, for health and safety reasons, a very directional antenna is used in this project apart from its need to meet the design requirements.

Although other radar types exist such as the pulse radar, pulse-doppler radar, continuous-wave (CW) radar and frequency modulated continuous-wave (FMCW) radar, the objective of this project was to design an FMCW radar showing a method of range detection; operating at a centre frequency of 900MHz, to detect a range of no more than 20m. It excluded any speed, size, shape, altitude, velocity, position measurements and programming. Although the proposed frequency and detection ranges were of the order of a tenth of that expected of a modern radar system, the design still demonstrated the basic mode of operation of a typical FMCW radar.

2 Literature Review

Radar technology is one major branch of radio frequency and microwave engineering which attracts government funding for various projects and research to ensure its rapid growth and development. Various types of radars exist; in the past, many similar projects have been carried out to find ways their design could be improved, some of these radar types are briefly discussed; their drawbacks are also pointed out to illustrate the reason for not being used to achieve the set goals for this project. The reason for choosing the FMCW type is also discussed alongside the reason for adding certain components which are not very common with such a radar type.

Radar Types Based on Radar Function

Radar sets are usually designed to either search for a target or having located one, track it. Radars that perform both functions are rare and require relatively more complicated circuitry; such radars usually have certain operational limitations.

Search Radar

Radars that go in search of specified targets are referred to as acquisition radars. When such a radar is used to search for a target, the radar operator does not know whether or not the target is in the area being searched. In a typical search radar, a large amount of space has to be covered and a systematic scan carried out. Consequently, fan beams are preferably used instead of narrow pencil scanning beams to ensure better coverage is achieved and the chance of missing the presence of a target is avoided [3].

Tracking Radar

A tracking radar cannot follow a target without locating it; hence a search radar is used initially to point out targets to the tracker. The tracker then uses the error signal produced at the receiver to know the targets path and move the tracker's motor in the required direction [4]. The future position of the target is known by using the coordinates provided by the search radar and could track in range, angle, doppler or within any combination [5]. A common example of a tracking radar is the surveillance radar used by intelligence agencies.

Radar Types Based on Signal Processing Technique Employed:

Four main radar types exist using this criteria, they include:

- Pulse Radar
- Pulse-Doppler Radar
- Continuous-wave Radar
- Frequency Modulated Continuous-wave Radar

Pulse Radar

A pulse radar pulse-modulates the generated transmitter signal before sending high energy, short pulses in the form of electromagnetic energy bursts when in search of a target. The receiver is then switched on immediately to await the echo while the transmitter is automatically switched off. Pulse radars are very efficient when it is difficult to identify which part of the receiver's reflected signal is for a particular part of the transmitted signal in a continuously running transmitter [6]. Pulse radars are the most common types of search radars but it has certain associated draw backs, namely:

1) As a result of using 1 antenna it is not a feasible technique for comparing transmitted signals with echoes when observing a target with relative motion making it almost impossible for detecting velocity since it is not instantaneous.
2) If the right pulse repetition frequency (p.r.f) is not chosen, measurement ambiguities would occur because the echo would not return before the transmission of the next pulse [7].

$$Pulse\ interval = \frac{1}{p.r.f} \quad (1)$$

Despite these two main drawbacks, the pulse radar is easily designed and effective in providing range measurements if the p.r.f is carefully chosen.

Pulse-Doppler Radar

A pulse-doppler radar is a pulse radar that utilises the doppler effect phenomenon to discriminate moving targets from stationary ones [8]. The p.r.f chosen for this type of radar is usually high enough to operate with no blind speeds from unambiguous doppler measurements making it suitable for measuring velocities of targets at the expense of being unsuitable for range measurements since high p.r.f would result in short pulse intervals leading to range ambiguities since an echo would not return before the next transmitted pulse[9].

Continuous-Wave Radar

Knowledge of the doppler effect principle is key to understanding how a continuous-wave (CW) radar works. A CW radar like every other radar has a transmit and receive section. Its transmitter continuously generates an unmodulated oscillating signal of known frequency before comparing it with its received echo via a duplexer since the transmitter and receiver are both on continuously unlike in the pulse radar where a switch is used instead. Duplexers are devices that allow bi-directional communications in a communication channel, operating over its designed frequency range. Examples include ferrite circulators and magic tees. CW radars give no range information due to the absence of modulation but they often prove useful for velocity measurements using equation 2 [10].

$$f_d = \frac{2.v_r.f_t}{c} \quad (2)$$

Where:

$f_d = Doppler\ frequency$
$f_t = frequency\ of\ the\ transmitted\ signal$
$v_r = velocity\ of\ the\ target$
$c = speed\ of\ light$

Frequency Modulated Continuous-Wave Radar

To use the CW radar for range measurement, a common theoretical suggestion is to use a timing mark on both transmitted and received signals; the more distinct the timing mark is, the more accurate the round trip time (RTT) measurement would be.

However, the FMCW radar is a good solution to obtaining range information of a target. Like the CW radar, it transmits a signal continuously. Its transmitted signal could be any signal ranging from a sawtooth, triangular or sinusoidal waveform as long as the fashion in which the signal's frequency changes is known and the signal is frequency modulated. They are more effective than CW radars when finding the range of stationary targets as a result of frequency-modulating its transmitted signal, making it the best approach for meeting the specification of this project.

The method of obtaining range using frequency modulation can be summarised graphically in the figure shown below.

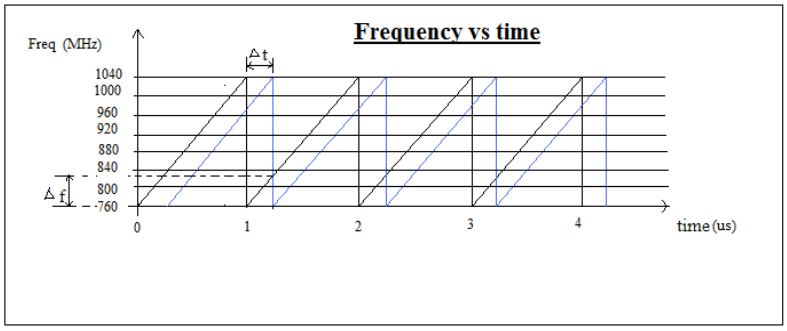

Fig 2.1: Sawtooth Frequency Modulation

In the figure, the black line represents the transmitted frequency-time relationship while the blue line represents the frequency-time relationship of the echo, which is a delayed version of the transmitted signal.

Thorough analysis of fig 2.1 shows that:

$$\Delta t = \frac{2R_{max}}{c};$$

$$m = \frac{\Delta f}{\Delta t};$$

$$\text{So that } m = \frac{\Delta f.c}{2m} \qquad (3)$$

Where:

$\Delta t = time\ delay\ between\ tx\ signal\ and\ echo$
$\Delta f = beat\ frequency, displaced\ on\ the\ frequency\ counter$
$R_{max} = maximum\ specification\ range$
$m = gradient\ of\ the\ freq\ vs\ time\ graph$
$c = speed\ of\ light$

The block diagram of the FMCW radar designed in this project is shown in fig 2.2; it consists of a Wilkinson power splitter (WPS), sawtooth generator, voltage controlled oscillator (VCO), circulator, an antenna, a mixer, quarter-wave (QW) transformer, amplifiers and filters.

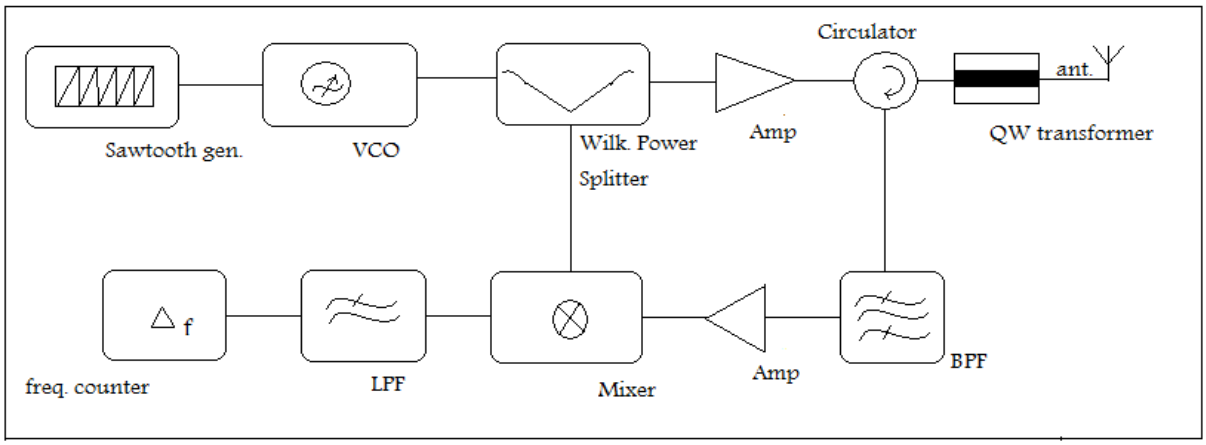

Fig 2.2 Block Diagram of an FM-CW Microwave Radar Range Detector

Using this design, any signal order than a sawtooth wave could be generated instead, provided the frequency of the chosen signal changes at a known rate. Through effective control of the gradient (m) of the frequency-time graph shown in fig2.1, an efficient radar would suffice since making m too high would result in little or no range detection and making m too small suggests very large periods which would make the detected round trip time negligible when compared, corresponding to a negligible beat frequency as well. Consequently, the gradient had to be chosen with precaution by choosing the frequency range from the VCO and the time period from the sawtooth generator carefully.

In the absence of a circulator, two separate antennas could be used as is usually the case; the drawback being that more components would need fabrication and less isolation would be achieved between the transmitter and receiver than when a duplexer is used with a single antenna.

Although some leakage signal should be permitted into the receiver to strengthen the echo, much care has to be taken to limit this leakage, to prevent the receiver from having its sensitivity degraded from physical damage through admitting excessive noise [11]. Therefore, the circulator used in the design avoided permitting unlimited leakage into the

receiver and at the same time, it did not provide perfect isolation between the transmitter and receiver.

Each block of the system's block diagram plays a vital role in ensuring the successful operation of the integrated radar set. All design methods and microwave engineering techniques behind the fabrication of each component are thus discussed, after a consideration of the system's link budget analysis and performance in chapter 3.

3 System design

3.1 Specification

The aim of the project was to design and implement a radar system illustrating the working principles of a typical radar, showing a method of range detection. It was aimed at showing a method of range detection, detecting a stationary car in the line of sight of its antenna of no more than 20m away with an operating centre frequency of 900MHz.

3.2 Link Budget Analysis

To achieve a given level of system performance, the size of the antenna, the transmitted power and signal to noise ratio (SNR) quantities were considered. The link budget identified the sources responsible for signal power attenuation and noise. Link budget analyses are usually done for radio communication systems that transmit over line-of-sight microwave and satellite channels [12]. At the end of the analyses, the transmit and receive powers were obtained and the SNR of the system calculated; hence, the systems performance was evaluated.

Expected Received Power (P_R):

The transmitted power (P_T) was estimated initially based on information from the data sheet of the VCO and amplifier. This estimate was evaluated as follows:

Output power from VCO ⟶ @ WPS ⟶ @ amplifier ⟶ @ antenna

{1.122mW} {0.56mW} {x100} {56mW}

From the inverse fourth power law, the received power was obtained using the formula below:

$$P_R = \frac{P_T G^2 \lambda^2 \sigma}{(4\pi)^3 R_{max}^4} \quad (4)$$

Where:

P_T= transmitted power = 56mW
G = gain of receiving antenna = 8.5dB = 7.1
λ = wavelength of the transmitted signal = 0.3m
R_{max} = maximum range =20m
σ = radar cross section of a car = 100m^2
P_R=Received power=80nW

Actual Received Power (P_R):

On testing the integrated system using a spectrum analyser, the received power was found to be -33dBm {501nW}; comparatively, this value was found to be greater than the expected

received power calculated using equation 4, where the radar was assumed to detect a target at maximum range. This result suggested that the radar set could detect the presence of a target and was expected since the room where the test was carried out was smaller than the specified maximum range of 20m.

In addition, the transmitted power was found to be 17.42dBm or 55.21mW confirming that the tests were carried out properly and the estimated transmitted power was logical.

3.3 Receiver sensitivity:

In the absence of noise in received signals, detection of any echo by the receiver would be possible no matter how weak [13]. Unfortunately, this is not the case in real-life applications as noise is admitted in practical receivers. The sensitivity of a receiver, simply put, is the minimum detectable signal (S_{min}) which would produce an output on the display. The sensitivity of superheterodyn receiver can be calculated using the formula:

$$S_{db} = -174_{dbm} + 10\log B_r + F_{db} \quad (5)$$

Where -174dBm is the KTB thermal noise floor in dBm derived at a room temperature of 290K, with 1Hz bandwidth. B_r is the receiver bandwidth which is 270MHz for this project and F_{db} is the noise figure of the receiver in dB, calculated shortly.

Noise Figure of the Receiver:

On hitting the target, the transmitted signal was attenuated and reflected back to the receiver section of the system via the circulator. The cascaded noise figure of the receiver was calculated using the formula:

$$F_{Cas} = F_1 + \frac{F_2 - 1}{G_1} + \frac{F_3 - 1}{G_1 G_2} + \cdots \quad (6)$$

Where 1, 2, 3... represent the position of the radar component from the antenna, on the receiver end.

Components Position from the Antenna	**Component**	**Gain(dB)**	**Operating Temperature, T_O (K)**	**Equivalent Temperature, T_e (K)**
1st	75Ω Coax	-2dB/ft	290K	300K
2nd	QW transformer	-4dB	290K	300K
3rd	50Ω Coax	-2dB/ft	290K	300K
4th	Circulator	-0.3dB	290K	300K
5th	50Ω Coax	-2dB/ft	290K	300K

Table 3.1: Parameters to calculate the noise figure

In general,

$$F = 1 + (L-1)\frac{T_e}{T_0}$$

$F_1 = 1 + (L_1 - 1)\frac{T_e}{T_0} = 1 + (1.58 - 1)\frac{300}{290} = 1.60$

**where L_1=1/G=1/$10^{-0.2}$=1.58

$F_2 = 1 + (L_2 - 1)\frac{T_e}{T_0} = 1 + (2.51 - 1)\frac{300}{290} = 2.56$

**where L_2=1/G=1/$10^{-0.4}$=2.51

Using the cascaded noise figure formula:

$$F_{cas} = 1.60 + \frac{2.56 - 1}{10^{-0.2}} + \cdots = 4.07 \; or \; 6.10dB$$

The first two terms in the cascaded noise figure equation are the most significant when compared to other terms in the formula as a result of the increasing number of divisors in the denominator. The calculated noise figure showed that the output SNR (SNR_{out}) was a fourth of the input SNR (SNR_{in}) since:

$$F = \frac{\mathrm{SNR_{in}}}{\mathrm{SNR_{out}}} \qquad (7)$$

In the future, to reduce the noise in the system, the feed from the antenna should be a rectangular wave guide (RWG) instead of coax as RWG is less lossy; coax was chosen however, as a result of its small size and ability to still meet the transmission line requirements.

Having calculated the noise figure, the receiver sensitivity was then calculated:

S_{db}= -174_{dbm}+10log (270MHz) +6.10dB

=-83.92dB or 4.05nW

A typical satellite communication link sensitivity is of the order of pW much smaller than the integrated system as the satellite receiver system needs to be more sensitive since its receiver signal is subject to all manner of losses, some of which are discussed next.

3.4 Range error and losses:

In radar systems, there are many sources of losses; some of which include RF losses, mismatch losses, beam shape collapses, operator and propagation losses. These losses, in most cases, lead to signal attenuation and in some other cases, range error.

Although filters were used at strategic points in the system, it was observed that it was impossible to completely cancel the effect of added noise because thermal noise is additive, white and Gaussian over all frequency. The added noise produced a random variation in the apparent amplitude of the echo. This amplitude variation due to noise affected the sawtooth-shape, making the target appear to be closer to the radar set than normal [14].

In typical radar systems, propagation losses are the most common loss sources as they are predominantly caused by atmospheric gases, especially oxygen and water vapour which absorb signals in significant amounts when compared to the rest [15]. Oxygen presents a two-way propagation loss of 0.04dB per nmi (1nmi=1852m) which turned out to be 0.0004dB for a maximum range detection of 20m and was thus ignored as a result of its insignificance.

Also, conductor losses due to frequency dependence and the effect of increasing surface roughness, dielectric and propagation losses at higher order modes lead to attenuation and losses in microwave transmission lines. Other sources such as transmission line losses, beam shape collapses, mismatch and operator losses are not discussed in detail in this report but an attempt was made to avoid them through the use of RF and microwave techniques such as quarter-wave matching, the use of good filters, properly shielded coax cables, and well-fabricated system blocks.

Transmission line losses virtually exist in all RF transmission lines except in impractical ideal lines. Table 2 summarises propagation and physical characteristics of some common transmission lines [16]. For this project, coax and microstrip lines were used for advantages shown in the table as well as their availability. Appendix I shows a mathematical analysis of the transmission lines used.

Characteristic	Coax	Waveguide	Microstrip	Stripline
Modes: Dominant/ Preferred Other	TEM TM &TE	TE_{10} TE & TM	Q-TEM Hybrid TM & TE	TEM TM, & TE
Dispersion	None	Medium – in band	Low	None
Bandwidth	High, DC-	Low, 1 octave	High	High
Loss	Medium	Low	High	High
Power Capacity	Medium	High	Low	Low
Size	Medium - Large	Large	Small	Medium
Manufacturing ease	Medium	Medium	Easy	Easy
Component integration	Hard	Hard	Easy	Moderate

Table 3.2: Propagation and Physical Characteristics of Transmission Lines

For this project, two computer packages namely, AWR's microwave office and Agilent's Advanced Design Software (ADS) were used to design the microstrip-line based components. Using the 'Tx line' function in AWR, the lengths and widths of the transmission line were obtained. The computer package used fundamental RF microstrip equations shown in appendix I to derive the required lengths and widths.

For instance, when the 'Tx line' function was used to obtain the length and width of a 50Ω microstrip line, the obtained length and width were 60.70mm and 2.4040mm respectively; when the formulae in appendix I were used on the other hand, the calculated length and width were 60.92mm and 2.424mm respectively; showing that the Tx line approximation is not far off from the calculated theoretical value.

Appendix I [17] shows a brief mathematical analysis of the transmission lines used while appendix II [18] contains information on the derivation of return and insertion loss; appendix III [19] shows relevant information relating to the Yagi-Uda antenna designed and appendix IV shows a table containing information outlining the characteristics of common substrate used in microstrip design [20].

4 Design Blocks

4.1 Sawtooth generator

Specification:

Since the 6-element Yagi antenna used had a fractional bandwidth of 30% of its operating frequency, its bandwidth was 270MHz from 765-1035MHz. Thus, the VCO had to be tuned using an appropriate input sawtooth waveform; so that the output fitted into the bandwidth of the antenna with a centre operating frequency of 900MHz.

In order for the radar to detect and indicate a beat frequency at the frequency counter, the sawtooth generator was to generate a wave having a time period of at most 1000ns i.e. T 1000ns because for a maximum detection of 20m, a time delay of 133ns is required; since,

——— (8)

*Where T=intended period of the generated sawtooth wave=**133ns***
R_{max}*=20m*

Ideally, T should be 133ns but in practice, a sawtooth generator fabricated using lumped elements usually has difficulty meeting such requirements as a result of these elements not going below a certain operational value due to drifts in component values over time and temperature, limiting the accuracy; hence the range 'T 1000ns'.

Solution:

Many valid ways of meeting the specification exist. One method is by using direct-digital synthesis (DDS) devices, where the embedded system-based sawtooth generator is programmable requiring no external components to set the frequency. It does this by loading onboard phase registers and involves continuous digital to analogue conversion using a chip to output a sawtooth; although this method seems attractive, in-depth knowledge of the chip's architecture is required and programming would be involved going beyond the scope of the project. To remain within the scope of the project however, the circuit in fig 4.1 was used to meet the requirements.

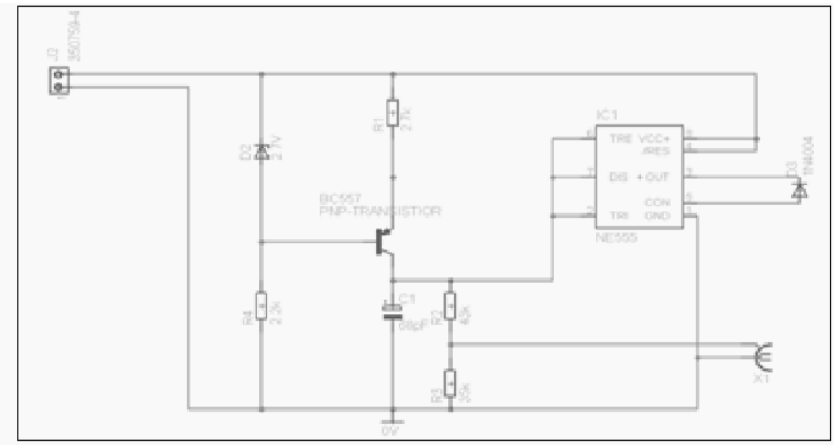

Fig 4.1 Schematic of the Sawtooth Generator

The circuit consists of an NE555-timer microchip configured for sawtooth generation. The part of the circuit consisting of a capacitor, resistor, zener diode and BC557 transistor form a current source that charges and discharges the capacitor, forming a sawtooth waveform across the capacitor. On supplying the circuit with 5V, a sawtooth wave with Vpp=4.12V was observed on an oscilloscope; to meet the specification of fitting the frequency modulated signal in the bandwidth of the antenna, the Vpp was attenuated to 2.24V to ensure that appropriate voltage-frequency mapping between 760 to 1040MHz was achieved.

PCB Manufacture:

On completion of the schematic using EAGLE, the corresponding PCB board file was generated; fig 4.2 shows the PCB layout produced using the software.

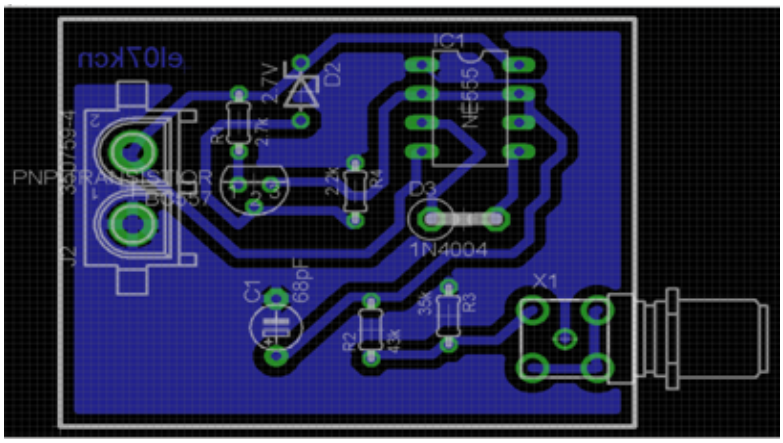

Fig 4.2: PCB layout of sawtooth generator schematic

FR4 was used as the substrate since it is cheap with good insulation and is hardwearing making it easy to replace components whenever necessary [21].

Before sending the single-sided PCB file for fabrication, the offset, track width and spacing were specified for ease of soldering components. Their values were chosen as $600\mu m, \geq 1mm$ and $\geq 800\mu m$ respectively to make soldering easier. A common ground was also used.

Fig 4.3 shows the oscilloscope trace of the output waveforms from the sawtooth generator on powering it up.

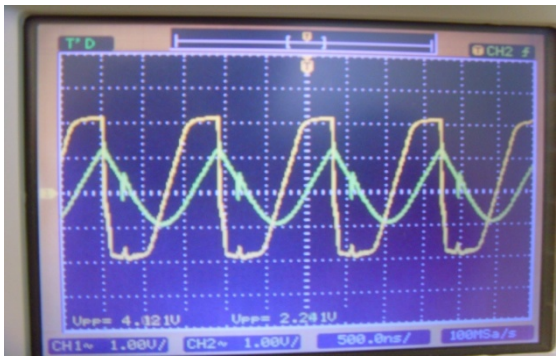

Fig 4.3: Oscilloscope trace of the sawtooth generator waveforms

4.2 Voltage controlled oscillator

Specification:

The transmitted signal with a centre operating frequency of 900MHz must fit in the bandwidth of the antenna given that frequency modulation is used. The generated frequency-modulated signal should be stable and controllable.

Solution:

The generated sawtooth signal had a frequency of approximately 1MHz; to successfully detect range, this signal had to be frequency-modulated by mapping its voltage values to frequency before amplification and broadcast. A surface mount VCO {minicircuit ROS-1250W-119+} was used to achieve this because like every crystal VCO, it maintained low phase noise, allowed low pulling and aqueous washing, and maintained high levels of frequency stability and control over a specified frequency range. Experience gained from working with such devices show that surface-mount technology-based devices are usually chosen over through-hole based technology because fewer holes need to be drilled through their boards and when defective, they are easier to be replaced.

To check that the previously existing voltage controlled oscillator worked properly, it was tested. Circuit connections were made using information from table 4.1.

Pins	**Label**	**Impedance/Line Width**
10	RF OUT	50Ω/2404μm
14	Vcc	NA/NA
2	Vtune	NA/NA
1, 3,4,5,6,7,8,9,11,12,13,15,16	Ground	Ground Plane/NA

Table 4.1: Pin Connections of the VCO {ROS-1250W-119+}

Fig 4.4 shows the PCB layout of the VCO mount board drawn using AWR [22]; ADS could also be used for this purpose.

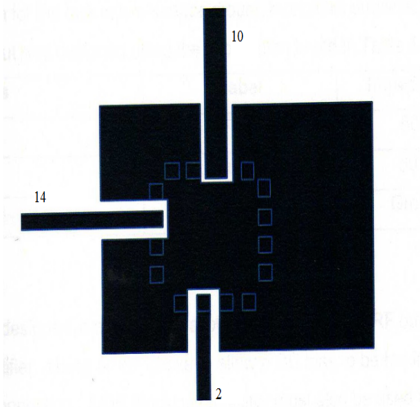

Fig 4.4: Pin Layout of the surface mount VCO

On testing the device with the sawtooth generator, the following result was obtained; it is shown graphically in fig 4.5 for the input tuning voltage from 0V to 2.24V.

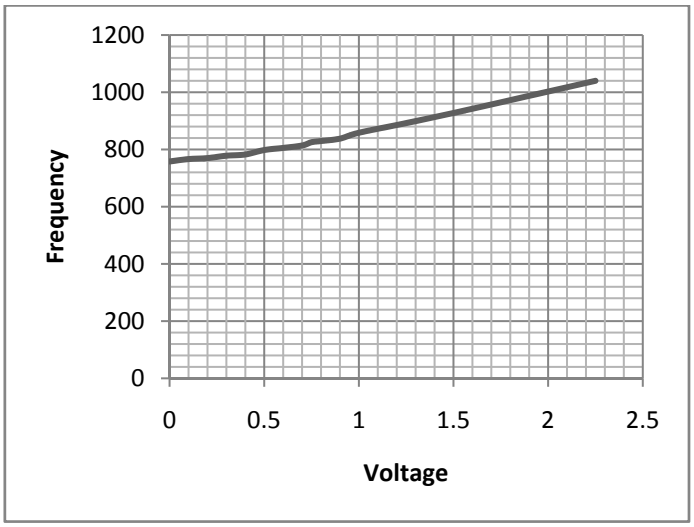

Fig 4.5: Performance Curves obtained on testing the VCO.

The above result was obtained at room temperature using a HP8593E spectrum analyser.

4.3 Wilkinson Power Splitter

Specification:

From the block diagram in fig 2.2, at the midpoint of the transmitter, a reference signal was required as a local oscillator for the mixer in the receiver to enable comparison between the transmitted signal and the received signal at the receiver end.

Solution:

A 3-port Wilkinson power splitter was used to meet the requirement because unlike other 3-port power splitters such as the lossless T-junction divider, and the resistive divider, it achieves isolation between its matched output ports while being lossless [23]. Although the Wilkinson power divider could be made to give any power division, a microstrip 3dB WPS shown in fig 4.6 was fabricated.

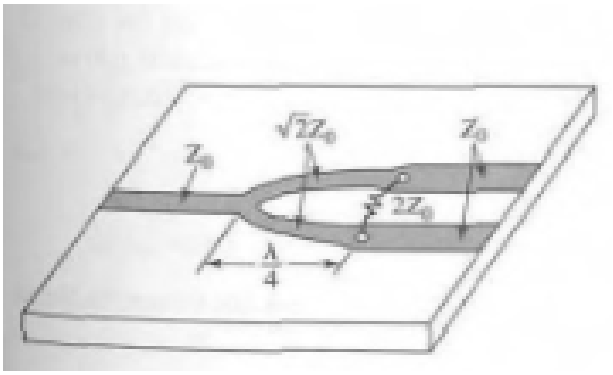

Fig 4.6: A typical 3-port Microstrip Wilkinson Power Splitter

Where in fig 4.6:

$Z_0=50\Omega$; and $2Z_0=100\Omega$;

$Z_a=\sqrt{2}\ Z_0=\sqrt{2}\ (50)=70.71\Omega$;

$\lambda=c/f=3x10^8/900x10^6=0.3m$;

$\lambda_{eff}=\lambda/\sqrt{2.2}=0.3/\sqrt{2.2}=0.202m$; $\lambda_{eff}/4=0.202m/4=59565\mu m$

Using the AWR Tx tool, the lengths and widths of the 50Ω and 70.7Ω lines were obtained.

Impedance(Ω)	Length (µm)	Width (µm)
50 Ω	10000	2404
70.71 Ω	61721.9	1365

Table 4.2: AWR Tx line Lengths and Widths for the WPS

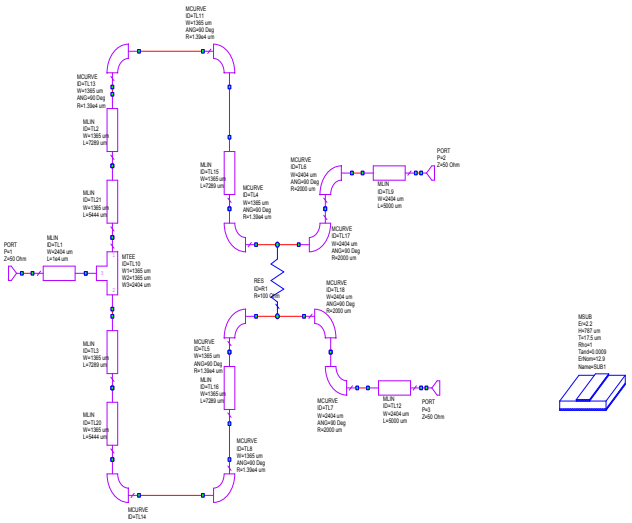

a) AWR Schematic of the WPS

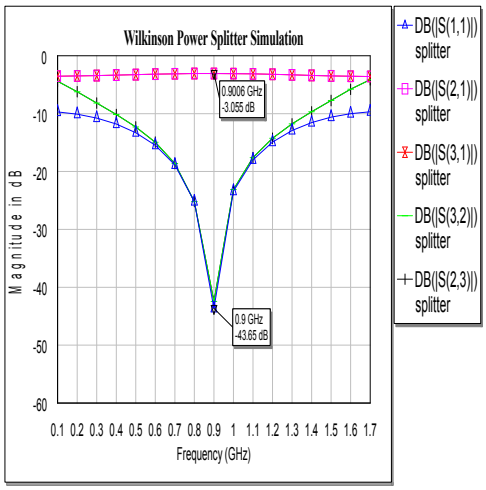

b) AWR Simulation of the WPS

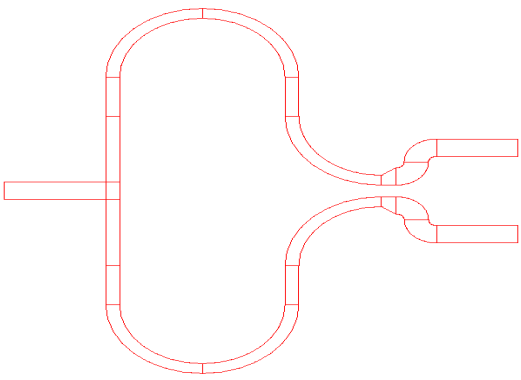

c) PCB Layout of the WPS

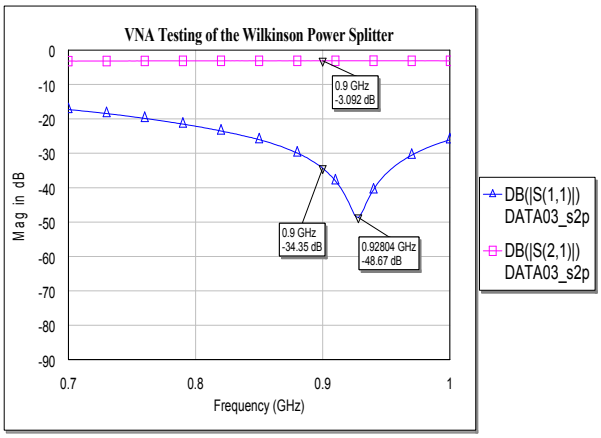

d) VNA test result of the fabricated WPS

Fig 4.7: AWR Simulation and VNA Test of the Wilkinson Power Splitter

On testing the WPS, on the VNA, a slight shift was observed; this shift was ignored since a significant return loss of -34.35dB was still achieved at 900MHz. Like in the AWR simulation (fig 4.7b), the VNA test result (fig 4.7d) showed that a forward transmission of minus 3dB (-3dB) was achieved leading to 50% division of the input power. Bended microstrip branches were used instead of straight branches like in the theoretical case to achieve compactness and prevent coupling of signals on the fabricated device.

Simulating the WPS using AWR showed that S_{31} was same as S_{21} as expected in a Wilkinson divider from knowledge of its S-matrix; therefore, all similar S-parameter plots have been omitted to avoid unnecessary repetition. The S-matrix of an ideal Wilkinson splitter is given by:

$$[S] = \frac{1}{\sqrt{2}}\begin{bmatrix} 0 & j & j \\ j & 0 & 0 \\ j & 0 & 0 \end{bmatrix} \quad (9)$$

Using the appropriate 100Ω-isolation resistor matched the network ports; the quarter-wavelength-long line served as a quarter-wave transformer to match the 50Ω-load impedances to the 100Ω resistor; with identical potentials on all terminals, there will be zero power loss within the resistor [24]. The value of the chip resistor does not affect the input matching although its value is important to minimise reflections for input signals [25].

4.4 Amplifiers

Specification:

Since the transmitted signal was to be transmitted through a noisy channel, it required amplification before transmission as well as on reception of at the receiver.

Solution:

Much care is needed in amplifier design as slight errors introduce a significant amount of noise and instability to the system. It is often preferable to design for a lower gain and wider bandwidth as it is easier to stay within tolerance limits. Hence there is always a trade-off between gain and bandwidth when designing an amplifier. The smith chart is a useful graphical tool to aid the design of an amplifier; as it enables the use of constant gain, noise and stability circles.

For precision and simplicity, the amplifiers chosen for the amplification of the signals on transmission and reception were minicircuit surface mount monolithic amplifiers {MAR-6SM+} operating from dc to 2GHz. Both have a 20dB gain and 3dB noise figure. The pin layout of the amplifier is shown in table 4.3.

Pins	Label	Impedance/Line Width
1	Radio Frequency(RF) input	50Ω /2.404mm
3	RF output & DC input	50Ω /2.404mm
2,4	Ground	Ground Plane / NA

Table 4.3: Pin Connections of amplifier {MAR-6SM+}

Fig 4.8 shows the PCB layout for mounting the surface mount amplifiers [26].

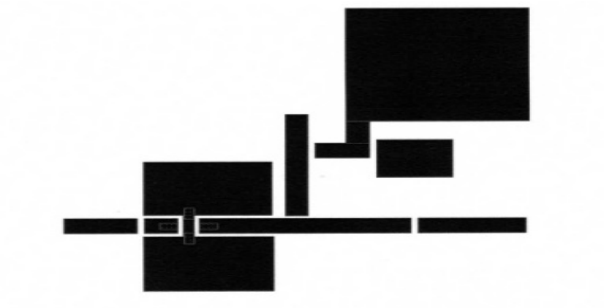

Fig 4.8: Pin Layout of the surface mount amplifier

The PCB mount board had both input and output DC blocking capacitors to cut off DC components; and an RF choke was used in series with the V_{CC} bias resistor to minimise the effect of the bias resistor on the performance of the amplifier.

4.5 Circulator

Specification:

Since a single antenna was used for reasons already discussed in section 2, some means of power flow from the end of the transmitter to the beginning of the receiver section had to be created.

Solution:

Solid-state ferrite circulators whether clockwise or anticlockwise, are widely used duplexers; resonant cavity waveguide systems and diode-limiters are other common examples. For this project, a clockwise microwave SMA C-975/250-X circulator was used to meet the specification as a result of its suitable operating frequency range (850-1100MHz), 50Ω impedance, VSWR of 1.2, 0.5dB insertion loss and direction of power flow from port 1 to 2 on transmission and from port 2 to 3 on reception. Fig 4.9 shows the diagram of a typical clockwise circulator showing the direction of power flow.

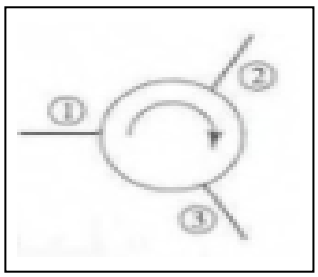

Fig 4.9: Diagram of a clockwise circulator

Ferrite circulators in general, have a decoupling of at most 40dB and can therefore not protect highly sensitive receivers from high transmit powers sufficiently; However, they are good for radars with low transmit powers. An ideal clockwise circulator has an S-matrix of the form:

$$[S] = \begin{bmatrix} 0 & 0 & 1 \\ 1 & 0 & 0 \\ 0 & 1 & 0 \end{bmatrix}$$

This S-matrix pointed that the device was not a reciprocal one and would allow power to flow in only one direction as a result. To obtain the S-parameter of an anticlockwise circulator, the port indices of a clockwise circulator is transposed; to achieve this in practice, the polarity of the ferrite bias field is reversed [27]. Junction and waveguide circulators exist but have the same operating principle. Terminating the 3rd port in an internal 50Ω load would give an isolator but it is not discussed since it was not used in the project.

4.6 Antenna

Specification:

To successfully detect the target, a single transmit-receive antenna was required. This antenna was to have very good directivity, have sufficient operating bandwidth, provide sufficient gain, and have a radiation resistance of preferably 50Ω; where a 50Ω antenna is not achieve, it needed to be matched to the rest of the system at least.

Solution:

A good antenna design can improve the overall system performance in a wireless communication system. Consequently, the right choice had to be made for the antenna-type used. Antennas are of various forms; they could be a piece of wire, an aperture, a lens, or a patch etc [28].

Aperture antennas are generally used for higher frequency transmission in the microwave spectrum (300MHz-300GHz). Horn antennas are aperture antennas with good gain and directivity; it is mostly found in air and space craft applications because they can be conveniently flush-mounted on the skin of such devices [29]. When working in the UHF range, aperture antennas require inconvenient large-sized waveguide apertures and as a result, it is not appropriate for short range detection especially for this system with operating frequency of 900MHz.

Microstrip antennas such as patch antennas are conformable to planar and non-planar surfaces [30], they are easy to manufacture and compatible with monolithic microwave integrated circuit designs. The drawback of this antenna is that performance prediction would be very difficult as a result of the complicated mathematical analysis behind its design. Its operational bandwidth is very narrow typically only a fraction of a percent.

Wire antennas are very simple to fabricate, they are made up of simple conducting wires, they could be of any chosen shape, they could be straight in the case of a monopole and dipole, or they could be in the shape of a loop or a helix. The drawback with this antenna type is that it does not provide an attractive gain or directionality for applications that are in dire need of directivity as they are almost isotropic.

Array antennas are used in applications that require radiation characteristics not achievable by a single element. It could be an aperture array, a Yagi-Uda array or a microstrip patch array. Depending on the number of elements used, such antennas could occupy large amounts of space; nevertheless, they are an attractive option for achieving good radiation patterns. For this project, a 6-element Yagi-Uda antenna array (fig4.10) was used; it consists of a single dipole antenna with an array of reflectors and directors adjacent to it. Yagi antennas as they

are often called, have an end-fire radiation pattern [31]; having 6 elements, the theoretical directivity of the fabricated antenna was roughly 6x1.5=9 i.e. 6 times that of a dipole; it was about 78% efficient, suggesting a gain of approximately 7; it had a fractional bandwidth of 30%, and an operating frequency of 900MHz, thus, its design met the antenna specification.

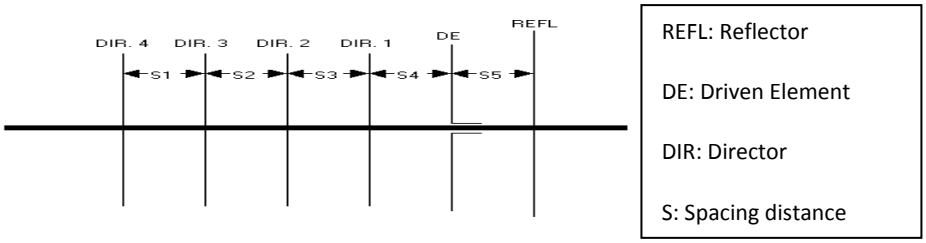

Fig 4.10: Yagi-Uda Array antenna

The fabricated Yagi antenna had a radiation resistance of 300Ω using a 300Ω-ladder line dipole based feed element; it was built on a plastic bar and held upright using a retort stand. It had to be transformed to 75Ω since a 300-75Ω balun and a 75Ω TV-coax were available; further transformation was done using a quarter-wave transformer to match the 75Ω cable to the rest of the 50Ω-circuitry. Like most antennas, it was either vertically or horizontally polarised depending on what position it was held in; this was not an issue however, since only one antenna was used. Appendix III shows the typical beam patterns of yagi antenna with different number of elements present.

When fabricating the antenna, the dipole element had to be connected to the balun using the shortest wire length possible to avoid creating unnecessary inductance which could disrupt the performance of the antenna. In the absence of an anechoic antenna test chamber, a vector network analyser was used to observe the S-parameters of the antenna. Fig4.11 shows the test result and confirms that the antenna worked in required frequency range and bandwidth judging from its S_{11} since it is found to be relatively low over the operating range.

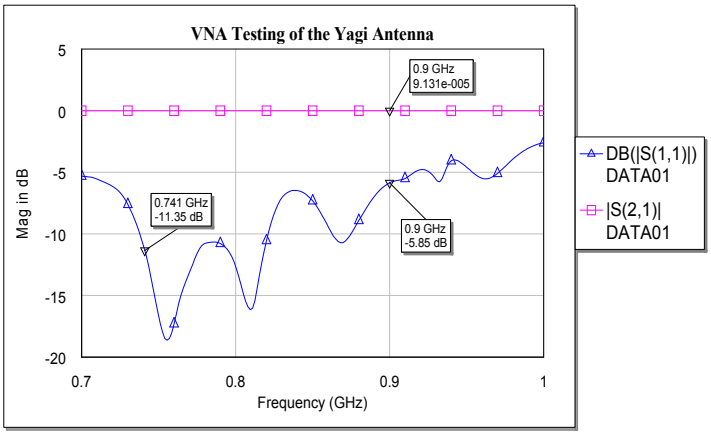

Fig 4.11: VNA test result of the antenna

Since the antenna was not powered but fed directly to the VNA an expected S_{21} of 0dB was observed. To fabricate a Yagi antenna operating at the correct centre frequency, the following formulae were used to obtain accurate lengths and spacings [32].

Lengths:

REFL=0.495 X λ_O

DE=0.473 X λ_O

DIR1=0.440 X λ_O

DIR2=0.435 X λ_O

DIR3=0.430 X λ_O

DIR4=0.425 X λ_O

Spacing:

S_1=0.25 X λ_O

S_2=0.25 X λ_O

S_3=0.25 X λ_O

S_4=0.125 X λ_O

S_5=0.125 X λ_O

Where:
$\lambda_O = \frac{C}{f} = 0.33m$

It should be noted, however, that in the absence of a yagi antenna other directional antennas such as dish antennas, backfires and panel antennas could be used. Omni-directional antennas are useful for Wi-Fi applications; such antennas include ceiling domes, mobile vertical antennas, vertical omnis and rubber ducks [33]. They are required for applications that require wide-coverage; hence they were not appropriate for the design.

4.7 Quarter-Wave Transformer

Specification:

To minimise input and output reflections during transmission and reception as a result of the 50-75Ω mismatch that existed between the circulator and the 75Ω cable, a matching technique was required.

Solution:

Although other techniques such as stub matching could have been used to meet the matching requirement, quarter-wave matching was chosen over it because of the fabrication complexities involved when using either short or open circuit stubs because wherever T-junctions exist in microstrip lines, the flow of current in such lines are distorted [34].

AWR Tx line tool provided information on the length and width of the line needed to manufacture the device via photolithography. On successfully manufacturing it, it was tested to observe its performance at 900MHz. Fig4.12 shows the physical layout of the transformer having a line impedance of $\sqrt{50 \times 75}\Omega$ since its load is wholly real using the formula:

$$Z_T = \sqrt{Z_O \times Z_{IN}} \quad (10)$$

Fig 4.12: Physical Layout of the Quarter-wave Transformer

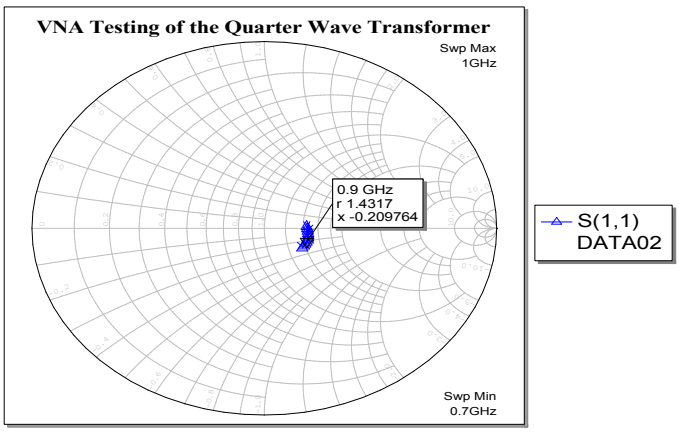

Fig 4.13: VNA test result of the fabricated QW transformer

Fig4.13 shows the test result of the fabricated device, it showed that an acceptable band of frequencies were around the matched point of the smith chart meeting the specified design requirement.

As a result of dielectric discontinuities which occur in microstrip lines, different frequencies propagate at different speeds. At very high frequencies, the shift in distribution of the electromagnetic fields above and below the line results in a frequency dependent change in the line's propagation characteristic and impedance [35]. To minimise the chances of these lines radiating from any discontinuity, the circuit can be shielded, although in most cases, the shields help excite other resonant modes in the available cavities [36].

In the absence of the quarter-wave transformer in the circuit, the voltage reflection coefficient at the load (Γ) and VSWR (S) were calculated to be:

Voltage reflection coefficient

$$\Gamma = \frac{Z_L - Z_O}{Z_L - Z_O}$$

$$= \frac{75 - 50}{75 + 50}$$

$$\Gamma = 0.2 < 0^o$$

VSWR along the line:

$$\boldsymbol{S} = \frac{1+|0,2|}{1-|0.2|} = \mathbf{1.5}$$

Therefore, to minimise the effect of such reflections and improve the VSWR, a quarter-wave transformer was required. To confirm that the right characteristic impedance is obtained, the aspect ratio (w/h) and the relative permittivity of the substrate could be used to obtain the corresponding impedance by using a standard substrate characteristic graph containing aspect ratio, relative permittivity and characteristic impedance on 3 separate axes.

Lossy dielectric substrates and the finite conductivity of metals do not cause any significant changes to the characteristic impedance and operating wavelength of the microstrip, but they are responsible for the attenuation of signals in the line.

The attenuation quantity is related to other line characteristics via the formula [37]:

(11)

Where:

represents the attenuation due to dielectric losses

represents the effective dielectric constant

represents the speed of light

represents the loss tangent

4.8 Bandpass filter

Specification:

In order to regulate the frequency getting into the mixer, and isolate the received signal from added noise, a bandpass filter (BPF) was to be used on reception of the signal before immediate amplification since the received power was weak.

Solution:

Considering that ideal BPFs with brick wall transitions are inexistent, a Minicircuit BPF {VBFZ-925+} was used having a pass band of 800-1050MHz. The filters insertion and return loss responses are shown below.

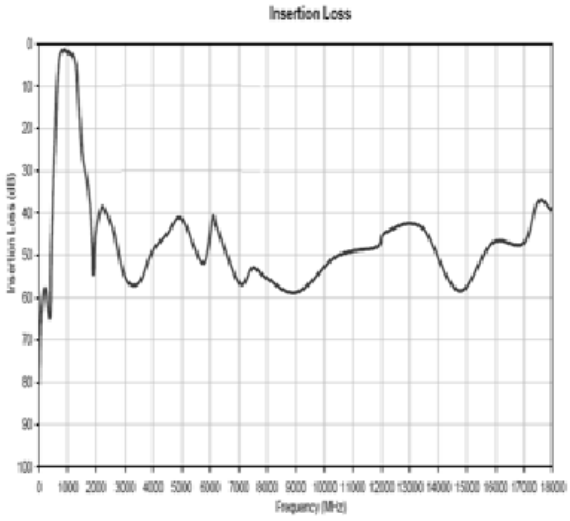

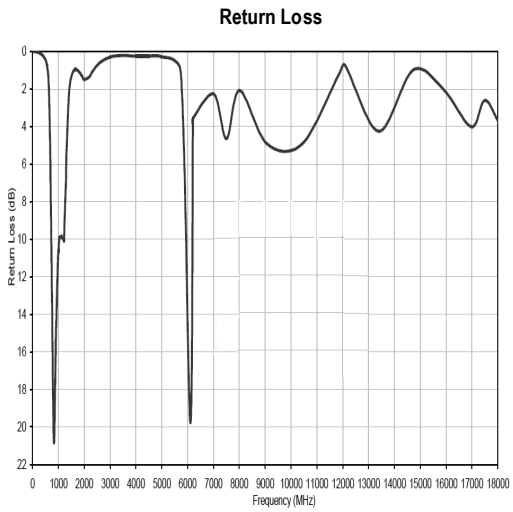

Fig 4.14: Performance Curves of the Bandpass filter

The chosen filter provided a 30dB rejection for unwanted frequencies, low insertion loss, excellent power handling, and great temperature stability.

A lumped element based filter could have been used to meet the requirements but on simulating the design on RF Sim99, the suggested lumped element values for the design were not readily available; in addition, lumped element filter design approach is not recommended for the design of UHF filters due to parasitic effects of inductors and capacitors that become pronounced at such high frequencies causing them to resonate with themselves.

Microstrip filters could also be used by intelligently separating adjacent microstrip lines. Such filters function by coupling their signals; however they do not offer low insertion losses or great rejection although they still isolate undesirable frequencies to some extent and thus, require careful fabrication to achieve such required precision.

The presence of the BPF between an antenna and the receiver prevented interference with any neighbouring transmit-receive devices and avoided amplifying unwanted signals which could cause problems within the receiver. Hence, a very good rejection filter such as the minicircuit coaxial filter had to be used.

4.9 Mixer

Specification:

A mixer was required after the amplifier and BPF at the receiver to provide the difference frequency required by the frequency counter.

Solution:

A high reliability minicircuit mixer {ADE-R5LH+} was used to obtain the intermediate frequency required because of certain features it possesses such as low conversion losses, and excellent LO-RF isolation. Study of its internal structure shows that it uses band stop filters, branch line couplers, RF shorting lines, diodes and open circuit termination to achieve effective mixing [38].

The pin layout of the mixer used is shown in fig4.15 and was drawn using AWR microwave office following study of the data sheet.

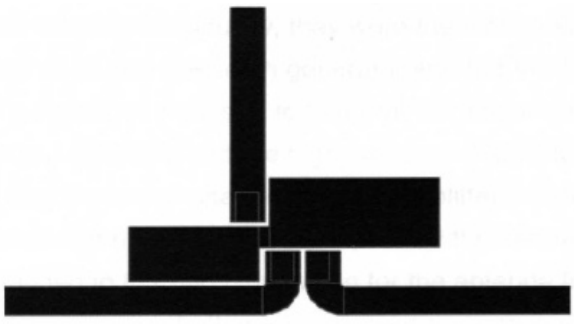

Fig 4.15: Pin Layout of the surface mount mixer

The local oscillator pin of the mixer was connected to one of the output ports of the Wilkinson power splitter (WPS) while the RF and IF pin were connected to the amplifier and

lowpass filter respectively; table 4.4 shows the pin layout of the mixer. The maximum power rating of the mixer is 50mW so the amplified power and WPS power had to be measured using the spectrum analyser, before being fed to the mixer. The measured amplifier and WPS powers were minus 3.57dBm (-3.57dBm or 0.44mW) and approximately 0.1mW respectively, both suitable for the mixer.

Pins	Label	Impedance/Line Width
6	Local oscillator (LO)	50Ω/2.404mm
3	Radio Frequency (RF)	50Ω/2.404mm
2	Intermediate Frequency (IF)	NA (Low freq required) / 2.404mm
1,4,5	Ground	Ground Plane/NA

Table 4.4: Pin Connections of mixer {ADE-R5LH+}

4.10 Lowpass filter

Specification:

The mixer's output frequency contained both the sum and difference of the two input LO and RF signals so a lowpass filter was required to isolate the needed beat frequency from the sum frequency.

Solution:

Again, various filter design techniques could have been employed to meet the design specification but the chosen lowpass filter (LPF) for this project was a coaxial LPF {BLP-30+}. It had a pass band from DC to 35MHz which was suitable for the design, and had a good insertion and return loss as shown in fig 4.16.

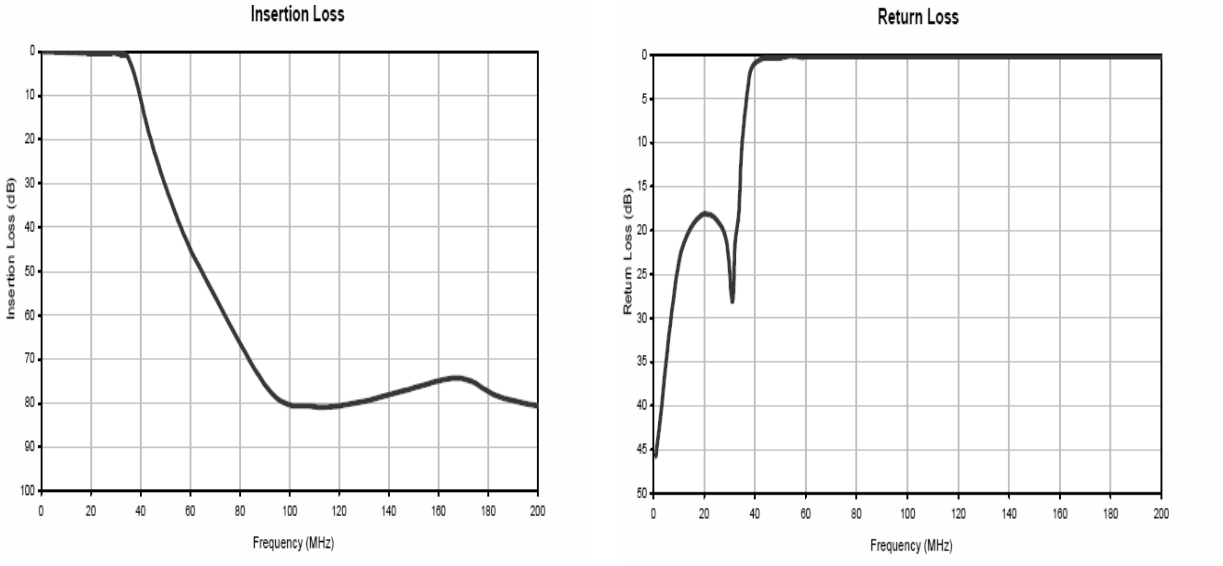

Fig 4.16: Performance Curves of the Lowpass filter

Referring to fig 2.1, the frequency modulation illustration; the following formula was derived:

Round-trip time (R_{TT}):

$$\frac{LPF\ cut\ off}{280MHz} \times 1\mu s = R_{TT}$$

For maximum range detection, the calculated R_{TT} was calculated to be 133ns {see section 4.1}

$$\frac{LPF\ cut\ off}{280MHz} \times 1\mu s = 133 \times 10^{-9}s$$

$$\therefore LPF\ cut\ off = 37.24MHz$$

Round-trip distance (R_{TD}):

$$R_{TD} = R_{TT} \times c = 133 \times 10^{-9}s \times 3 \times 10^{8} = 40m$$

Actual distance (d):

$$d = \frac{R_{TD}}{2} = \frac{40m}{2} = 20m$$

The estimated beat frequency of this radar was deduced to be at most 37.24MHz for maximum range detection; this estimated maximum beat frequency is the same as the required LPF cut-off, hence, the BLP-30+ filter was chosen.

4.11 Frequency Counter

Specification:

A visual display indicator was required to give range information on determining the presence of an echo.

Solution:

The most common radar indicator is a cathode-ray tube oscilloscope; four main presentations which include the A, B, C-scope and Planned position indicators exist and are used to display data of the target. To avoid going out of scope of the project, all programming and employment of embedded system design had to be excluded from the design.

A HP5340A frequency counter was used; it was chosen as a result of its availability and capability to detect frequencies up to 18GHz. The obtained beat frequency from the counter gave indirect information about the range of the target from the radar. Frequency counters that calculate the range automatically exist but are quite costly; hence the HP5340A type was chosen since it was readily available. Ideally, both physical quantities are related by the formula:

$$Range = \frac{f_{beat} \cdot c}{2m}$$

Alternatively,

$$Range = \frac{1}{2}\left(\frac{LPF\ cut\ off}{280MHz} \times 1\mu s \times c\right)$$

Where: *m=gradient of the freq-time graph in fig2.1=279.3×10^6/s^2*
c=speed of light; and f_{beat}*=beat frequency.*

5 System Integration and Testing

Each individual component was tested using a scope, spectrum analyser or voltage network analyser where applicable as briefly discussed in section3. Before integrating the entire system, as shown in the system block diagram; each subsection was tested before adding the next in order to be able to trace faults, if any, until the entire system in fig 2.2 was integrated and tested.

On testing the 5V powered sawtooth-VCO combination on the spectrum analyser, the corresponding frequency response obtained on the screen was found to fit in the antenna bandwidth with an output power of -1.80dBm close to the VCO output power on the datasheet. This signal was then connected to the WPS and by terminating one of the output ports with a 50Ω-termination, each output termination was tested. Observation showed that the output power was reduced to 50% its input value as the power level reduced to -3.60dBm at a slightly shifted frequency of 920MHz as expected from the slight shift observed when only the WPS was tested using the VNA.

The signal was then fed into one of the amplifiers and the power was found to increase by 20dB to 16.40dBm as suggested by the amplifier datasheet. The circulator and antenna were then added with the circulator's third port connected to the spectrum analyser; the displayed signal was found to be attenuated with noise added to it as expected. The BPF was then connected to this third port with one of its ends connected to the spectrum analyser, where a cleaner trace was observed.

Next, the cleaner signal was then amplified and fed into the RF pin of the mixer while the output of the initially 50Ω-terminated WPS was connected to the LO port of the mixer; the IF was observed on the spectral analyser where it was observed that the mixer produced both sum and difference frequencies. On connecting the lowpass filter, the sum frequency was removed and the difference frequency was found to shift depending on the movement of the antenna and what object it was pointing at since various objects in the room had different radar cross sections; the transmitted, received and intermediate signals obtained from the spectrum analyser are shown in fig 4.17(a), (b) and (c) respectively. The test result illustrated in (b) was obtained immediately after the bandpass filter while (a) is the transmitted signal after amplification via the circulator.

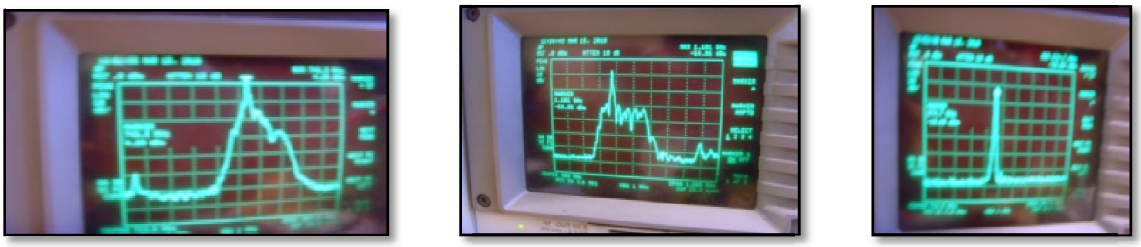

(a)The transmitted signal (b) The received signal c) The IF signal

Fig 5.1: Spectrum Analyser Test Results of the radar

Surprisingly, on connecting the lowpass filter to the frequency counter, the output on the frequency counter remained static at 10.01MHz irrespective of what direction the antenna was placed; This result suggested that a target approximately 5m away was detected.

Round-trip time:

$$\frac{10\text{MHz}}{280MHz} \times 1\mu s = 3.571 \times 10^{-8}s$$

Round-trip distance:

$$3.571 \times 10^{-8}s \times 3 \times 10^{8} = 10.714m$$

Actual distance:

$$\frac{10.714m}{2} \cong 5.36m$$

Further investigation carried out using an oscilloscope confirmed reception of a signal which varied on waving a metallic plate in front of the antenna; at this point it was then inferred that the problem occurred as a result of a malfunctioning frequency counter, and if replaced the radar would display readings correctly.

Recommendation:
In the future, any other input waveform with known rate of change order than a sawtooth generator could be explored to observe and compare the system's performance. Other high gain and more directional antennas such as mechanically-steered parabolic and horn antennas could be used and in addition, some embedded system design techniques could be included in the scope to convert the IF frequency from the LPF, to range.

To identify the target more easily and reliably, a transponder can be placed on the target to actively respond to incident 'interrogative' signals instead of relying on echoes which may be received from more than one target. This recommendation may not be well suited for a tight budget as it is expensive and may require large sized equipments.

6 Conclusion

This report has been used to discuss to a reasonable depth, the design processes involved in designing a FMCW microwave radar range detector. Although the specified design frequency of 900MHz and maximum range of 20m were much smaller than in practical radars, the aim of the design to demonstrate the mode of operation of typical FMCW radars was achieved.

The specified design frequency was slightly shifted on testing although it did not present significant changes to the system. The link budget analysis carried out provided information on the transmit and receive powers of the system as well as its signal to noise ratio (SNR);

The design decisions made throughout the project's duration showed foresight resulting in the detection of a beat frequency when tested on the spectrum analyser even though on testing the device on the frequency counter a static output was displayed. Frequency modulation was achieved and the overall performance illustrated the practicalities of RF and microwave engineering theories used throughout the entire project duration.

References

[1] SKOLNIK, M. *Introduction to radar systems*. New York: McGraw Hill, 1980.

[2] WORLD HEALTH ORGANISATION. Electromagnetic Fields and Public Health: *radars and human health* [online], 1999 [Accessed 31 March 2010], Fact sheet N°226. Available from: http://www.who.int/peh-emf/publications/facts/fs226/en/index.html

[3] WHEELER, G. *Radar Fundamentals*. New Jersey: Prentice-Hall, 1967.

[4] WHEELER, G. *Radar Fundamentals*. New Jersey: Prentice-Hall, 1967.

[5] SKOLNIK, M. *Introduction to radar systems*. New York: McGraw Hill, 1980.

[6] WHEELER, G. *Radar Fundamentals*. New Jersey: Prentice-Hall, 1967.

[7] WHEELER, G. *Radar Fundamentals*. New Jersey: Prentice-Hall, 1967.

[8] SKOLNIK, M. *Introduction to radar systems*. New York: McGraw Hill, 1980.

[9] WHEELER, G. *Radar Fundamentals*. New Jersey: Prentice-Hall, 1967.

[10] WHEELER, G. *Radar Fundamentals*. New Jersey: Prentice-Hall, 1967.

[11] SKOLNIK, M. *Introduction to radar systems*. New York: McGraw Hill, 1980.

[12] PROAKIS, J. 4ed. *Digital Communications*. New York: McGraw Hill, 2001.

[13] WHEELER, G. *Radar Fundamentals*. New Jersey: Prentice-Hall, 1967.

[14] WHEELER, G. *Radar Fundamentals*. New Jersey: Prentice-Hall, 1967.

[15] WHEELER, G. *Radar Fundamentals*. New Jersey: Prentice-Hall, 1967.

[16] STEENSON, D.P. *Microwave Transmission Lines*, lecture notes distributed in the topic ELEC3360 RF & Microwave Engineering. University of Leeds, 2 December 2009, not published.

[17] POZAR, D. 2ed. *Microwave Engineering*. New York: John Wiley & Sons, 1998.

[18] LUDWIG R., P. BRETCHKO. *RF Circuit Design; Theory and Applications*. New Jersey: Prentice-Hall, 2000.

[19] CARTER, R.G. *Electromagnetic Waves; Microwave Components and Devices* [online]. London: Chapman and Hall, 1990, [Accessed 4 April 2010]. Available from: http://www.cockcroft.ac.uk/education/Carter_EM_book/EM_Waves_PDF/CONTENTS.pdf.

[20] FOOKS E.H, R.A. ZAKAREVICIUS *Microwave Engineering using Microstrip circuits.* Australia: Prentice Hall, 1990.

[21] HAIKNEY G. , ELEC 3850, *The Design of a Microwave Radar Range Detector*, BEng dissertation, University of Leeds UK, 2009, not published.

[22] HAIKNEY G. , ELEC 3850, *The Design of a Microwave Radar Range Detector*, BEng dissertation, University of Leeds UK, 2009, not published.

[23] POZAR, D. 2ed. *Microwave Engineering*. New York: John Wiley & Sons, 1998.

[24] FOOKS E.H, R.A. ZAKAREVICIUS *Microwave Engineering using Microstrip circuits.* Australia: Prentice Hall, 1990.

[25] FOOKS E.H, R.A. ZAKAREVICIUS *Microwave Engineering using Microstrip circuits.* Australia: Prentice Hall, 1990.

[26] HAIKNEY G. , ELEC 3850, *The Design of a Microwave Radar Range Detector*, BEng dissertation, University of Leeds UK, 2009, not published.

[27] POZAR, D. 2ed. *Microwave Engineering*. New York: John Wiley & Sons, 1998.

[28] BALANIS C.A. 3ed. *Antenna Theory; Analysis and Design.* New Jersey: John Wiley & Sons, 2005.

[29] BALANIS C.A. 3ed. *Antenna Theory; Analysis and Design.* New Jersey: John Wiley & Sons, 2005.

[30] BALANIS C.A. 3ed. *Antenna Theory; Analysis and Design.* New Jersey: John Wiley & Sons, 2005.

[31] CARTER, R.G. *Electromagnetic Waves; Microwave Components and Devices* [online]. London: Chapman and Hall, 1990, [Accessed 4 April 2010]. Available from: http://www.cockcroft.ac.uk/education/Carter_EM_book/Carter_EM_book.html

[32] SKY SCAN. *Sky scan science awareness project website* [online]. 1999-2005. [Accessed 5 April 2010]. Available from: http://www.skyscan.ca/6_element_yagi.htm.

[33] RADIO LABS. *What is the best antenna for me?* [online]. 2003-2004. [Accessed 15 April 2010]. Available from: http://www.radiolabs.com/Articles/wifi-antenna.html

[34] FOOKS E.H, R.A. ZAKAREVICIUS *Microwave Engineering using Microstrip circuits.* Australia: Prentice Hall, 1990.

[35] FOOKS E.H, R.A. ZAKAREVICIUS *Microwave Engineering using Microstrip circuits.* Australia: Prentice Hall, 1990.

[36] FOOKS E.H, R.A. ZAKAREVICIUS *Microwave Engineering using Microstrip circuits.* Australia: Prentice Hall, 1990.

[37] FOOKS E.H, R.A. ZAKAREVICIUS *Microwave Engineering using Microstrip circuits.* Australia: Prentice Hall, 1990.

[38] FOOKS E.H, R.A. ZAKAREVICIUS *Microwave Engineering using Microstrip circuits.* Australia: Prentice Hall, 1990.

[39] SCOTT. *The Ultimate guide to 11m CB antennas* [online]. [Accessed 9 April 2010]. Available from: http://www.signalengineering.com/ultimate/yagi.html

[40] FOOKS E.H, R.A. ZAKAREVICIUS *Microwave Engineering using Microstrip circuits.* Australia: Prentice Hall, 1990.

Bibliography

Books:

COLLIN R.E, *Foundations for Microwave Engineering* Singapore: McGraw-Hill International, 1992.

CUTRONA, L. *Radar Handbook,* New York: McGraw-Hill Book Company, 1970.

EDWARDS T.C. *Foundations for microstrip Circuit Design* New York: John Wiley & Sons Ltd, 1981.

FUSKO V. *Microwave Circuits Analysis and Computer Aided Design* London: Prentice-Hall International Ltd, 1987.

HAGEN J. *Radio Frequency Electronics: Circuits and Applications,* New York: Cambridge University Press, 1996.

HUNTER I. *Theory and Design of Microwave Filter,* London: Institute of Electrical Engineers, 2001.

RIZZI P. *Microwave Engineering Passive Circuits* published by New Jersey: Prentice-Hall, 1998.

Journal:

BERIZZI, F. , M, MARTORELLA, M. BERNABO, *IET Radar, Sonar & Navigation: A range profiling technique for synthetic wideband radar*, Oct 2008, Vol. 2 Issue 5, p334-350.

Websites:

Argos Press Pty Ltd *Ian Faulconbridge's website* [online] [Accessed 5 April 2010]. Available from: http://www.argospress.com/Resources/radar/

HOLLMANN, M. *Dr. Hans E. Hollmann's website* [online]. 2001. [Accessed 5 April 2010]. Available from: http://www.radarworld.org/

P-N DESIGNS, *Radars* [online] [Accessed 5 April 2010]. Available from: http://microwaves101.com/

The Aerospace Corporation. *Radar [*online]. 1995-2008. [Accessed 5 April 2010]. Available from: http://aerospace.org/

Appendix I

Coax

The Inductance per unit length is given by: $L = \frac{\mu}{2\pi}\ln\frac{b}{a}$ H/m

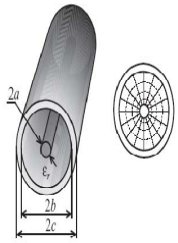

Coaxial cable cross section

The Capacitance per unit length is, $C = \frac{2\pi\varepsilon'}{\ln\frac{b}{a}}$ F/m

The Resistance per unit length is given by:

$R = \frac{R_S}{2\pi}\left(\frac{1}{a}+\frac{1}{b}\right)$ Ω/m , where $R_S = \frac{\rho}{\delta_S}\Omega$, and $\delta_S = \sqrt{\frac{2\rho}{\omega\mu}}$

Where, R_S, is surface resistance of the conductors and δ_S is the skin depth.

The conductance per unit length is, $G = \frac{2\pi\omega\varepsilon''}{\ln\frac{b}{a}}$

The useful frequency limit for the dominant TEM mode in coax is given by the onset of the next higher mode, which is given by the cut-off of the TE_{11} mode, or,

$$f_C = \frac{c}{\pi(a+b)\sqrt{\mu_r\varepsilon_r}}$$

Microstrip

$$\frac{w}{d} = \begin{cases} \dfrac{8e^A}{e^{2A}-2} & for\ w/d < 2 \\ \dfrac{2}{\pi}\left[B-1-\ln(2B-1)+\dfrac{\varepsilon_r-1}{2\varepsilon_r}\left\{\ln(b-1)+0.39-\dfrac{0.61}{\varepsilon_r}\right\}\right] & for\ w/d > 2 \end{cases}$$

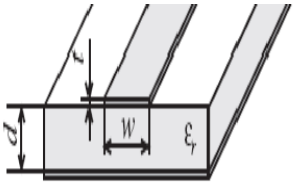

Microstrip conductor layout

Where,

$$A = \frac{Z_0}{60}\sqrt{\frac{\varepsilon_r+1}{2}}+\frac{\varepsilon_r-1}{\varepsilon_r+1}\left(0.23+\frac{0.11}{\varepsilon}\right) \quad and \quad B = \frac{377\pi}{2Z_0\sqrt{\varepsilon_r}}$$

$$\varepsilon_{eff} = \frac{\varepsilon_r+1}{2}+\frac{\varepsilon_r-1}{2}\frac{1}{\sqrt{1+12d/w}}$$

$$Z_0 = \begin{cases} \dfrac{60}{\sqrt{\varepsilon_{eff}}}\ln\left(\dfrac{8d}{w}+\dfrac{w}{4d}\right) & for\ \dfrac{w}{d} \le 1 \\ \dfrac{120\pi}{\sqrt{\varepsilon_{eff}}\left[w/d+1.393+0.667\ln\left(w/d+1.444\right)\right]} & for\ \dfrac{w}{d} \ge 1 \end{cases}$$

Where:

$$\beta.l = \left(k_o\sqrt{\varepsilon_{eff}}\right).l$$

$$k_o = \frac{2\pi f}{c}$$

Appendix II

Return Loss {RL}

Return Loss is the loss obtained due to power reflection in discontinuous transmission lines which in most cases is as a result of a mismatch in the line. It could be expressed in term s of reflection coefficient.

$$RL = -10log\frac{P_r}{P_i} \quad (12)$$

$$= -10log|\Gamma_{in}|^2$$

$$RL = -20log|\Gamma_{in}| \quad (13)$$

Also,

$$RL = -ln|\Gamma_{in}| \quad (14)$$

Insertion Loss {IL}

Insertion Loss is the decibel representation of transmission coefficient between points in a transmission line circuit

$$IL = -10log\frac{P_t}{P_i} \quad (15)$$

$$IL = -10\log\frac{P_i - P_r}{P_i} \quad (16)$$

$$= -10log(1 - |\Gamma_{in}|^2)$$

$$IL = -20log|T|; \text{ and} \quad (17)$$

$$T = 1 + \Gamma = 1 + \frac{Z_1 - Z_0}{Z_1 + Z_0} = \frac{2.Z_1}{Z_1 + Z_0} \quad (18)$$

Where:

P_r represents the reflected power

P_t represents the transmitted power

P_i represents the incident power

Γ_{in} represents the input reflection coefficient

T represents the transmission coefficient

Appendix III

Yagi-Uda Antenna used:

The electric field:

$$E = E_0 \frac{1-e^{Nj\psi}}{1-e^{j\psi}} \quad (19)$$

$$|E| = |E_0| \frac{\left|Sin\frac{N\psi}{2}\right|}{\left|Sin\frac{\psi}{2}\right|} \quad (20)$$

Where:

$$\psi = kdcos\theta + \alpha$$

And zeros occur at:

$$\psi = \frac{2\boldsymbol{\pi}}{\boldsymbol{N}}, \frac{\boldsymbol{4\pi}}{\boldsymbol{N}}, \frac{\boldsymbol{6\pi}}{\boldsymbol{N}}\ \boldsymbol{etc}$$

And maxima occur at:

$$\psi = \frac{3\boldsymbol{\pi}}{\boldsymbol{N}}, \frac{\boldsymbol{5\pi}}{\boldsymbol{N}}, \frac{\boldsymbol{7\pi}}{\boldsymbol{N}}\ \boldsymbol{etc}$$

For End-Fire Array:

$$\alpha = -90^o\ and\ d = \frac{\lambda}{4}$$

For Broad-side Array:

$$\alpha = 0^o\ and\ d = \frac{\lambda}{2}$$

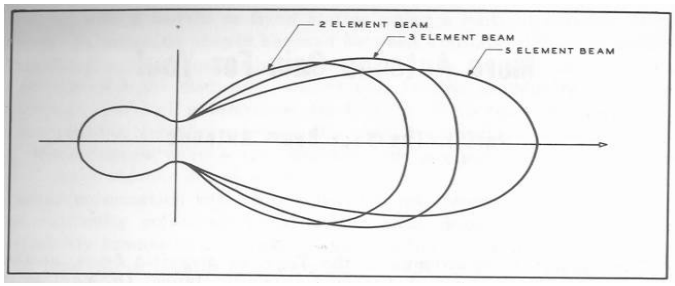

Typical Beam patterns of Yagi antennas with increasing number of elements [39]

Appendix IV

The Properties of some substrate materials

Material	ε_r	tan δ	Advantages	Disadvantages	+Notes
Air	1.0006	≥ 0	Pure TEM wave. Assumed as free space	No support for strip. Large physical size	
PTFE	2.1	0.0003		High Thermal expansion. Poor mechanical properties	
Reinforced Plastics	2.3-2.6	<0.001	Improved mechanical properties. Large Sizes-Low cost.	High Thermal expansion. Variability between branches	
Quartz	3.78	0.0001	Reproducible substrates. Useful in the mm range. Low thermal expansion		
Ceramic loaded plastics	2.5-10	<0.002	Good mechanical properties	variability between branches	
Alumina 99.5% pure	9.8	0.0001	Reproducible substrates-improving with purity.	Brittle. Slightly Anisotropic	1
Sapphire Al_2O_3	9.4 11.6	0.0001		Anisotropic crystal. Small size- high cost	2
GaAs	12.9	0.002	integration with high frequency active components	Thin substrates	3
	85	0.004	Reduced size components	Rough Surfaces. Temperature sensitive ε_r	4

+Notes [40]:

1) Readily available and popular substrate materials;
2) The cut with the C-axis normal to the ground plane gives electrical properties that are independent of the direction of propagation across the substrate. For electric fields along the C-axis, ε_r=11.6;
3) Tan δ<0.001 for the high resistivity material
4) A negative thermal coefficient of permittivity.

Recall the references for the appendices from section 3.4:

- Appendix I [17]
- Appendix II [18]
- Appendix III [19]
- Appendix IV [20]